Nuclear Medicine Image Registration by Spatially Noncoherent Interferometry

Christian Scheiber, Yann Malet, Gabriel Sirat, and Daniel Grucker

Institut de Physique Biologique, Faculté de Médecine, Université Louis Pasteur, Strasbourg; and CDO-Optimet, Paris, France

This article introduces a technique for obtaining high-resolution body contour data in the same coordinate frame as that of a rotating γ camera, using a miniature range finder, the conoscope, mounted on the camera gantry. One potential application of the technique is accurate coregistration in longitudinal brain SPECT studies, using the face of the patient (or "mask"), instead of SPECT slices, to coregister subsequent acquisitions involving the brain. **Methods:** Conoscopic holography is an interferometry technique that relies on spatially incoherent light interference in birefringent crystals. In this study, the conoscope was used to measure the absolute distance (Z) between a light source reflected from the skin and its observation plane. This light was emitted by a 0.2-mW laser diode. A scanning system was used to image the face during SPECT acquisition. The system consisted of a motor-driven mirror (Y axis) and the γ-camera gantry (1 profile was obtained for each rotation step, X axis). The system was calibrated to place the conoscopic measurements and SPECT slices in the same coordinate frame. **Results:** Through a simple and robust calibration of the system, the SE for measurements performed on geometric shapes was less than 2 mm, i.e., less than the actual pixel size of the SPECT data. Biometric measurements of an anthropomorphic brain phantom were within 3%–5% of actual values. The mask data were used to register images of a brain phantom and of a volunteer's brain, respectively. The rigid transformation that allowed the merging of masks by visual inspection was applied to the 2 sets of SPECT slices to perform the fusion of the data. **Conclusion:** At the cost of an additional low-cost setup integrated into the γ-camera gantry, real-time data about the surface of the head were obtained. As in all other surface-based techniques (as opposed to volume-based techniques), this method allows the match of data independently from the dataset of interest and facilitates further registration of data from any other source. The main advantage of this technique compared with other optically based methods is the robustness of the calibration procedure and the compactness of the sensor as a result of the colinearity of the projected beam and the reflected (diffused) beams of the conoscope. Taking into account the experimental nature of this preliminary work, significant improvements in the accuracy and speed of measurements (up to 1000 points/s) are expected.

Key Words: brain; registration; surface matching; SPECT

J Nucl Med 2000; 41:375–382

In many clinical situations, there is a need for precise anatomic localization of tracer distribution, for example, to pinpoint a tumor and follow its evolution after treatment. Epilepsy is another well-known condition requiring the accurate registration of scans recorded under different biologic conditions (ictal/interictal scans) (*1*). When an organ such as the brain is studied, both morphologic and functional data are required. These are inherently of a very different nature and can be obtained through different medical investigations, each yielding specific information that must be matched. The so-called multimodality approach has led to improved diagnoses, better surgical planning, more accurate radiotherapy, and countless other medical benefits. But this approach makes it necessary to register and merge data from different origins (MRI, SPECT, electroencephalography, magnetoencephalography) acquired in very different conditions. Even state-of-the-art single-photon nuclear medicine does not provide anatomic details with sufficient precision. Over the years, a broad range of registration techniques has been developed to suit various types of data (*2,3*). The method of choice was usually specific to the registration problem, but an ideal method would not be dependent on the data and could be used as a common reference to register different imaging or nonimaging sources. Such a method of choice would have to be precise and also robust to be compatible with different clinical situations. The equipment would have to be affordable and ready to use. In a large number of medical situations requiring precise localization and modality-to-patient registration (*4*), body contour can be used as a common reference. Unfortunately, body contour is not always available with adequate precision. This is the case in nuclear medicine, so that a second method must be used, such as a transmission scan or optical methods. This article reports the use of a miniature range finder that records the shape of the body within ±1 mm. To demonstrate the potential clinical usefulness of this method we chose 1 possible medical application: the registration of 3-dimensional data from the face, to be used as a common reference surface for the registration of brain morphologic imaging or functional data (or both). The key point of this approach is that the range finder can be calibrated so that both the SPECT slices and data about the face are in the same coordinate frame. Calibration is the critical step in this

Received Oct. 24, 1998; revision accepted Apr. 12, 1999.

For correspondence or reprints contact: Christian Scheiber, MD, Institut de Physique Biologique, Faculté de Médecine, UPRES-A 7004 CNRS, 4 rue Kirschleger, Strasbourg Cedex, F-67085 France.

approach. One advantage of this technique is the mounting of the device directly onto the γ-camera gantry, which simplifies the procedure.

MATERIALS AND METHODS

A miniature range finder mounted on the γ-camera gantry measured the distance between a light source on the skin and the observation plane. The light source was obtained by the reflection on the skin of the light emitted by a green laser diode. A scanning system (a mirror driven by a galvanometer) was used to scan a profile of the face while the γ camera was acquiring data in a step-and-shoot mode. The process was repeated for each rotation step of the SPECT acquisition procedure. At the end of the process, a mask of the human face was reconstructed, in which spatial resolution was a function of the angular division of the rotation, the number of data points recorded for each profile, and the range covered by the scanning system. After mechanical and optical calibration, the "mask" data were in the same coordinate frame as the SPECT slices. The mask was then used to register the nuclear medicine data.

Conoscopy is a simple implementation of a specific type of polarized light interference process. In its simplest implementation, conoscopy uses a single crystal with its optical axis parallel to the geometric axis of the system. Briefly, conoscopic holography (*5*) is an interferometry technique that relies on spatially incoherent light interference resulting from the use of birefringent crystals. The recorded interference pattern is a Fresnel zone pattern that consists of a set of concentric black and white fringes. The interfringe decreases with distance from the center of the zone according to the formula (see below). A conoscopic probe consists of a birefringent crystal sandwiched between 2 polarizers (Fig. 1).

A primary beam issued from the object passes through the first circular polarizer, which generates 2 orthogonally polarized π/2 phase-shifted secondary beams that penetrate the crystal. According to classic optics, such an anisotropic crystal displays 2 specific modes of propagation, depending on the polarization of the incoming beam. In the "extraordinary" mode the refractive index depends on the angle between the beam and the optical axis of the crystal. In the "ordinary" mode the refractive index is constant. In other words, the beams in conoscopic systems follow the same optical path within the crystal but propagate at different speeds. Setting up the second polarizer to restore the diffracted beams in the same polarization mode allows them to interfere. At some point Q in the recording plane located at a distance r from the hologram center, the phase difference is given by (*6*):

$$\Delta\phi = (2\pi/\lambda)K(r^2/Zc^2),$$

where K is a crystal parameter and Zc is the conoscopic distance, a measure of the distance between the emitting point and the recording plane. The hologram is a light-intensity representation of the phase difference.

In the simplest conoscopic system, a single-light point is created on the object by a thin pencil of light. The hologram is recorded by a linear charge coupled device array, digitized, and processed. The methods to retrieve the point longitudinal position from the data have been reported (*7*).

Experimental Setup

The conoscopic probe and a laser diode were mounted on an aluminum arm that was attached to the gantry of a Helix 2-head γ camera (Elscint, Haifa, Israel), as shown in Figure 2 and in schematic diagrams in Figure 3.

This setup allowed the 2 γ-camera heads to move freely during acquisition (body contour) without interfering with the conoscopic measurements. The system can be easily mounted or dismounted from the γ camera, which was also used for routine clinical work.

Data from the conoscopic probe were digitized by a personal computer acquisition card. The holograms were further processed on a personal computer (Hewlett-Packard Co., Andover, MA). Dedicated acquisition and display programs were developed (MATLAB 5.2; The MathWorks, Inc., Natick, MA). The light source was provided by a diode-pumped green laser.

Acquisition Parameters

For all studies, a 180° rotation of the gantry with 3° steps was used. For conoscopy, 60 profiles (128 data points/profile, 20 points/s) were obtained; whereas for SPECT, 120 2-dimensional projection sets (2 heads, 128 × 128, zoom 1.5, pixel size = 2.01 mm) were acquired and reconstructed using filtered backprojection.

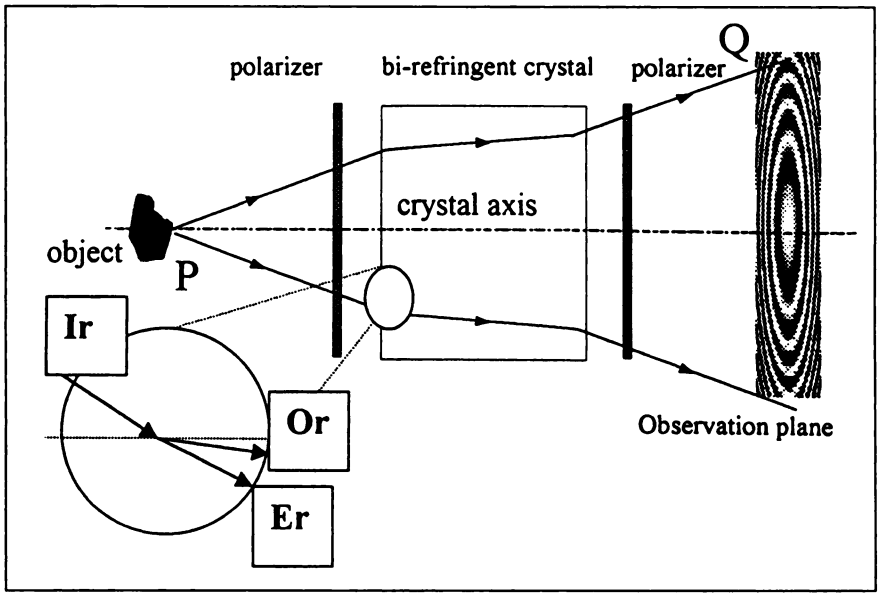

FIGURE 1. Interferometric basic setup. Incident ray (Ir) coming from P is polarized, then split into extraordinary (Er) and ordinary ray (Or) in birefringent crystal. After recombination, rays interfere on observation plane (Q). Distance PQ is derived from hologram.

FIGURE 2. Prototype of conoscopic system was mounted on gantry without disturbing radial motion of heads.

Calibrations

The critical point for a study such as this is the calibration procedure. First, the conoscopic measurements must be calibrated to take into account the distortions yielded by the scanning system used. Then a second calibration procedure is needed to refer the conoscopic data to the γ-camera coordinate frame. The scanning procedure yields a curved profile of a planar object (Fig. 4A). There are 3 sources of distortion in the evaluation of the distance between the conoscopic probe and the object. The first results from the use of a mirror. This distortion is intrinsic to the system and can be corrected, provided the scanning procedure is symmetric. The second type of distortion arises from the fact that the incident beam does not strike the rotational axis of the mirror, resulting in distortions that vary as a function of the angle of rotation of the mirror. The third kind of distortion arises from the offset of the angle formed by the incident beam and the mirror. The offset is equal to 0 in the initial position of the mirror (e.g., 45°) and varies as a function of the angle of the mirror during the scanning procedure. To quantify all these distortions, we used as a reference a wooden plane placed perpendicular to the axis of the beam. The solution adopted consists in correcting numerically the data measured. The reconstruction method makes use of landmarks to construct a calibration curve Z(F), where F is fringe number. This curve yields the distance Z between the object surface and the hologram center as a function of F, which includes all distortions. For all points other than landmark points, depth estimation is achieved by polynomial interpolation. Once performed, this calibration need not be carried out again. Figures 4A and B show the same data, before and after correction, respectively. The residual error is within 1 mm SD.

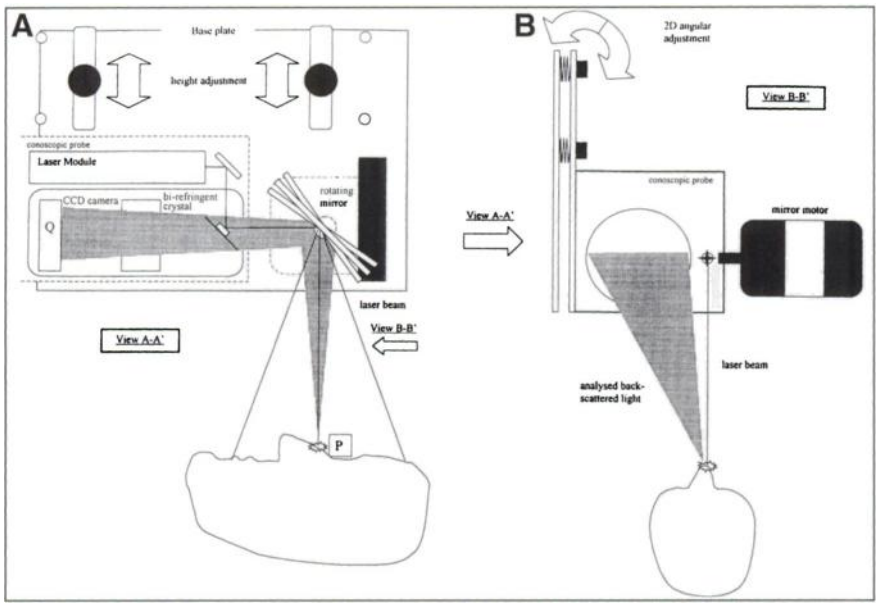

FIGURE 3. Schematic diagrams of experimental setup. (A) Distance was measured from emitting point on skin (P), reflected from green laser diode (0.2-mW power deposition) to observation plane (Q). CCD = charge coupled device. (B) Profile (128 points) of face was obtained with rotating mirror used as scanning system. Several paths for different mirror rotations are shown.

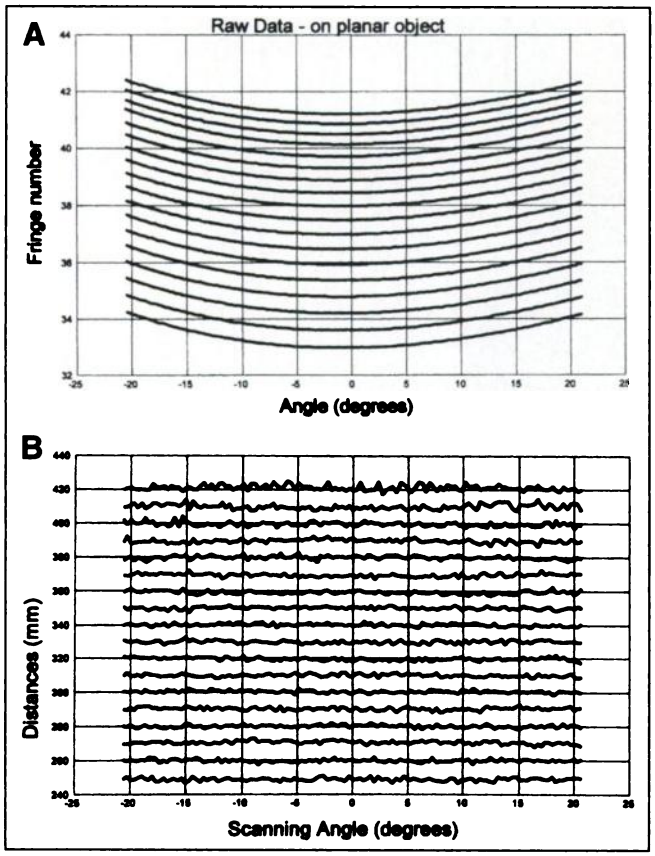

FIGURE 4. (A) Set of calibration curves of planar object at various distances expressed in number of hologram fringes, showing distortions, including curvature resuting from scanning method (−25° to +25°). (B) Same set of curves after calibration. Distances are expressed in millimeters, and distortions have been corrected.

Calibration of the Conoscopic Measurements with Reference to the γ Camera

With XY as the image plane axes and Z as the through-plane axis (along the main axis of the γ camera), the origin of the conoscopic measurement was set at the center of the acquisition volume. For the Z axis, the scanning system was tuned so that the laser beam would aim at the center of the field of view of the γ camera.

The conoscopic probe was mounted and tuned in such way that the laser beam was orthogonal to the γ-camera head (90° offset in the conoscopic data with reference to the SPECT data). For these preliminary measurements, the error was estimated to be within ±1°. For nuclear medicine data, this would result in a systematic rotation error of the mask, for which corrections could be made on the basis of experimental results on test objects. To this end, 4 lines, 1-mm deep and 25-cm long, were carved in the wall of a hollow aluminum rod that was positioned along the axis of rotation of the γ camera. The rod was subsequently filled with ^{99m}Tc (line source), and SPECT data were acquired. The centroid of the position of the image of the rod was used to ensure that the rod was at the center of each reconstructed image. The calibration tool ensured that the laser beam (0.5-mm wide) targeted the lines carved in the rod at 0°, 90°, 180°, and 270° (Fig. 5). After completion of this mechanical tuning, conoscopic acquisitions of the rod were made for quality control. The calibration procedure is an iterative process and needs to be done only once. Each time the conoscopic system was mounted on the γ camera, however, fine tuning was necessary.

To calibrate the Z axis, a 22-cm-diameter cylinder filled with a solution of ^{99m}Tc (74 MBq) was placed at the center of the field of view. Two 1-mm catheters were glued onto the surface of the cylinder and filled with a solution of ^{99m}Tc with an activity/mL 10 times that of the cylinder. SPECT acquisitions were made to ensure that the first catheter was in the 64th transaxial plane and the other in the 100th. The precise location of the catheters was then obtained with the optical system, which allowed tuning of the mechanical offset of the scanning system.

RESULTS

Conoscopic Measurements

Tests on Simple Geometric Forms. After calibration, conoscopic measurements were obtained on test objects in simulated clinical conditions. Measurements on a cylinder (22-cm diameter) showed a ±1% geometric distortion contour in the field of view of the scanning system. A

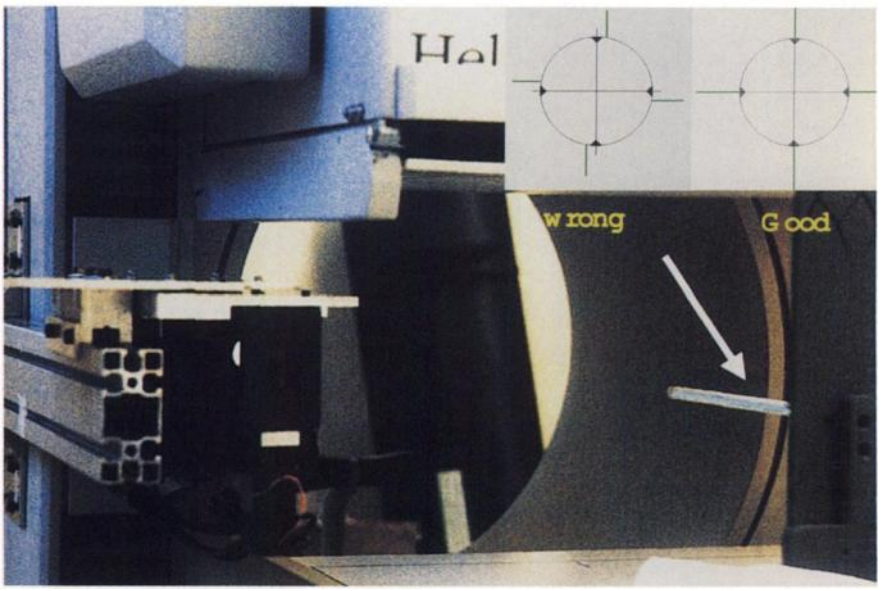

FIGURE 5. XY calibration procedure using rod (10-mm diameter, 25-cm long) at mechanical center of rotation of γ camera. Central cavity was filled with ^{99m}Tc and used to mark center of rotation.

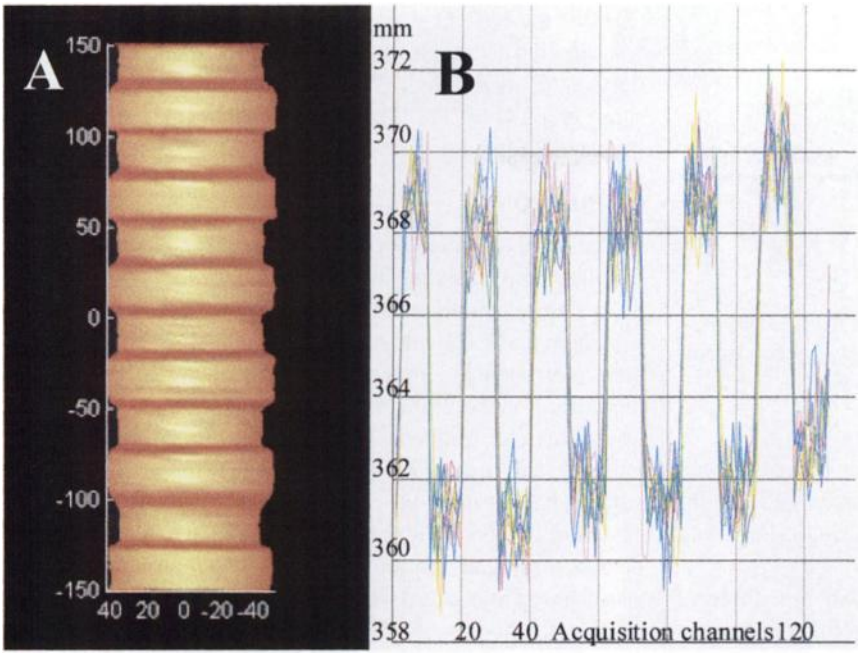

FIGURE 6. (A) Carved wooden bar (25-mm wide, 5-mm-deep notches) at 45° angle was used to confirm accuracy of calibration. (B) Conoscopic profiles obtained (mean, 5.1 ± 0.7 mm) after corrections.

25-mm-wide wooden ruler with 5-mm-deep notches (Fig. 6A) was positioned at a 45° angle. The mean depth measured was 7.2 ± 0.7 mm (Fig. 6B), resulting in a corrected value of 5.1 ± 0.7 mm ($7.2 \cos \pi/4 = 5.1$).

Brain Phantom. A 3-dimensional anthropomorphic brain phantom, referred to as Oscar, was used (JB005; NucleMed SA, Roeselare, Belgium). Oscar consisted of 40 plates stacked in a reproduction of the human head (Fig. 7A) The plates were glued together and cast with a high-quality, see-through polymer. For this experimental work, Oscar was coated with foundation cream (Fig. 7B), and conoscopic measurements ("mask") were performed in clinical conditions (Fig. 7C). Biometric parameters associated with Oscar and results measured with the conoscope are provided in Table 1. The height and depth were measured with reference to a sagittal or coronal plane at the same level and selected on visual inspection. The error was larger than that found for the biparietal and bicanthal diameters or the mouth; the limits of these parameters were clearly recognizable on the mask.

Registration of Mask and Brain Perfusion SPECT. Oscar was filled with a ^{99m}Tc solution (200 MBq). SPECT or conoscopic measurements were performed in various orientations similar to those encountered in clinical conditions. Once properly calibrated, the SPECT slices and the mask were in the same coordinate frame and were scaled so that they could be plotted on the same graph. The results are provided in Figure 8 with 3 different views of a 3-dimensional surface rendering of the Oscar mask and

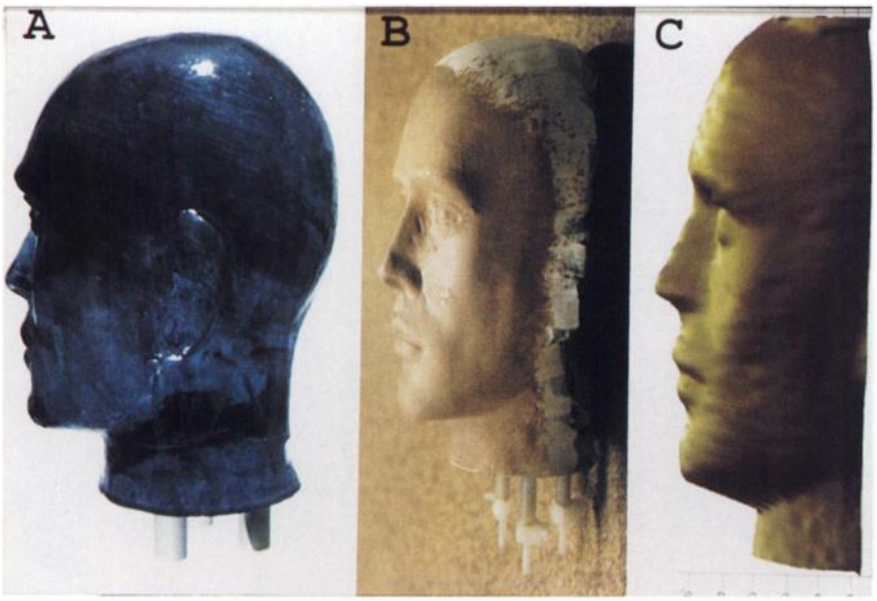

FIGURE 7. (A) Brain phantom consists of 40 plates glued together and cast in see-through polymer. (B) Test object was coated with foundation cream to facilitate measurement. (C)Three-dimensional surface rendering of phantom.

TABLE 1
Measurements of Mask Data with Reference to Oscar

	AP diameter (mm)	Biparietal diameter (mm)	Bicanthal diameter (mm)	Mouth width (mm)	Height (mm)
Oscar	130	166	80	58	142
Mask	124	161	78	56	135
Relative error (%)	4.6	3	2.5	3.5	5

AP = anteroposterior; mouth = mouth of Oscar; Oscar = 3-dimensional anthropomorphic brain phantom; mask = conoscopic measurements.

the 3-dimensional graph of the 40 isocontour curves derived from the SPECT study acquired simultaneously. The isocontour curves were obtained using a Matlab single-threshold routine).

The optical properties of the human skin are different from those of the cream-coated brain phantom, and humans usually have hair. For this preliminary study 1 volunteer was investigated. Two independent brain studies were performed 30 and 90 min after injection of ^{99m}Tc-ethyl cysteinate dimer (740 MBq). For the second scan, the volunteer was repositioned on the couch. The variations in the position of the head, although not actually measured, very likely included both a different tilt and rotation. The 3-dimensional representation of the second dataset is shown in Figure 9. The mask exhibited artifacts resulting from hair and had to be excluded from further processing.

One of the goals of this registration method was to use the mask instead of SPECT slices to merge images. This part of the work is in progress. But as a beginning, the rigid transformation that allowed the best superimposition of the second mask on the first (taken as a reference) was obtained manually, on the basis of the visual inspection of the 3-dimensional display (Fig. 10).

After the best fit was obtained, the rigid transformation was applied to the second set of SPECT slices, and the 4 datasets (2 masks and 2 SPECT slices) were plotted on the same graph (Fig. 11). The same process was applied to the human data (data not shown).

DISCUSSION

The goal of this work was to obtain, by means of a distance map, relevant information from the surface of the head, while simultaneously performing another examination, here a SPECT study. It is expected that the role of intra- and intermodality image matching in clinical work will increase. For the brain, which would be the major application, intrinsic methods using patient properties are less harmful and might be preferred to extrinsic ones. Skin surface-based methods have several attractive features: They are independent of the data of interest (here the count distribution) and require much less computing time than voxel-based methods. Unfortunately, nuclear medicine emission data cannot be used with appropriate resolution for the purpose of registration, so that another system must be used in conjunction with a γ camera. When available, transmission data could be used to derive body-contour information, but the spatial resolution remains a function of the physical characteristics of the γ camera, and such information is not acquired simultaneously with SPECT data. The use of intermediary systems to record surface data for image registration is well known. More specifically, optical systems have been used for transcranial magnetic stimulation localization (*8*) and SPECT/MRI registration (*9*). The originality of our work lies in the integration of this new miniature range finder onto the γ camera, which results in a simpler calibration procedure.

Moreover, the apparatus can be easily mounted and dismounted. The miniaturization of the device makes the system compatible with everyday work. The use of a range finder relying on optical principles has several advantages.

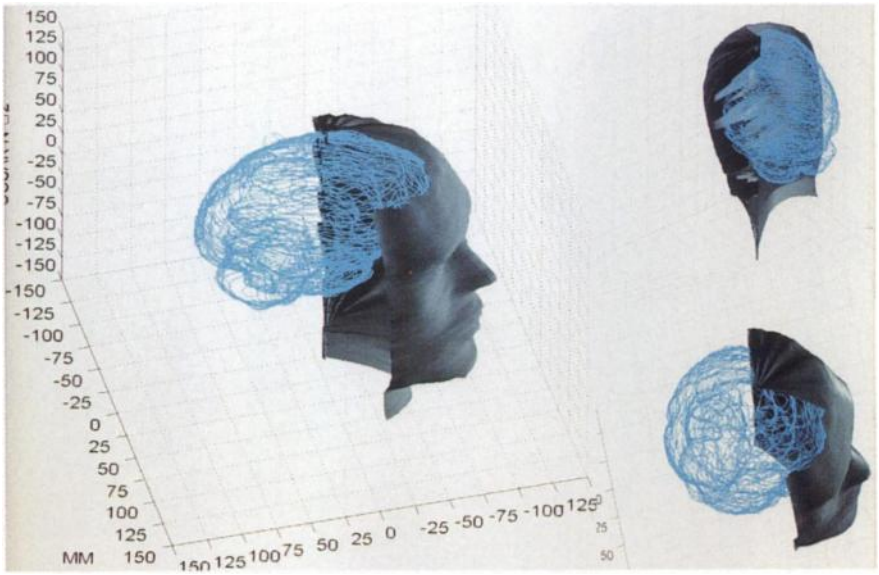

FIGURE 8. Three-dimensional surface renderings of SPECT and mask data acquired simultaneously, scaled and plotted on same graph. If calibration is accurate, images are registered without additional manipulation.

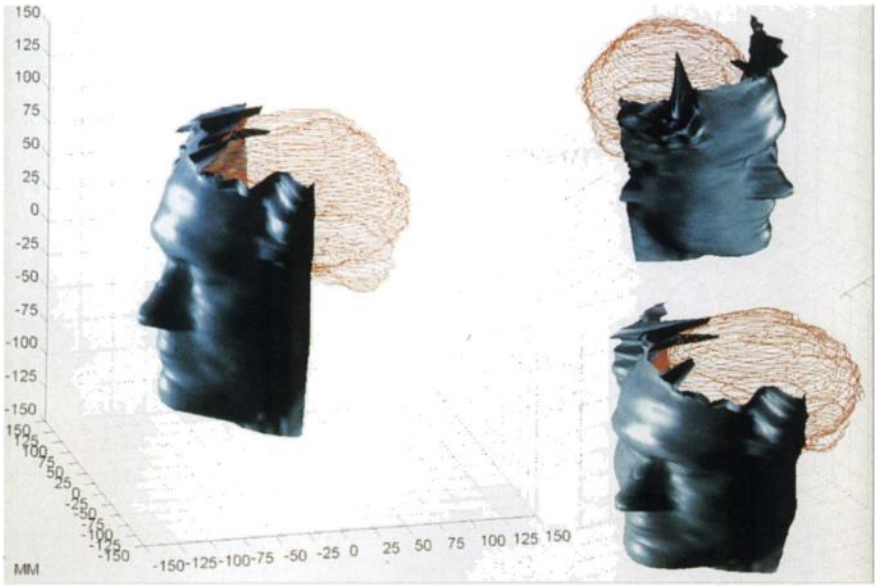

FIGURE 9. Three-dimensional views of volunteer. Note acceptable representation of face. Hair is not observable by conoscopy, thus yielding artifacts, so area must be excluded before further processing of mask data.

The acquisition rate can be high (theoretically up to 1000 points/s), which means that it would allow motion to be detected during the acquisition procedure, yielding high spatial precision. Another advantage is that the method is completely independent of the nuclear medicine acquisition process. In addition, once the system is properly calibrated, the principle allows the direct registration of mask and SPECT slices

Calibration is the key point of the method. The calibration files showed very little drift as a function of time. Despite the fact that the procedure was carried out manually, residual errors were within the range of the pixel size.

The quantitative measurement of registration accuracy is a difficult task (*10,11*). For this preliminary work, the geometric distortions of the face of the brain phantom were measured and judged acceptable. The registration of the 2 sets of data are given as an example of what could be expected from the method. The fusion of the mask and SPECT data was achieved by visual inspection only, and no registration error was measured. At this stage, we have begun to implement existing registration methods based on skin surface, which allow the registration of 2 heads from 2 imaging modalities (*12*). The next step is to implement the industrial version of the conoscope, equipped with a beam collinear with the measurement axis and fully integrated electronics allowing the output of Z measurements in real time, at a rate exceeding 100 points/s. Additional research work is necessary to implement a fully automated calibration procedure.

We have been able to mount and dismount and calibrate the system within 30 min because of the robust mechanical mounting of the device on the γ-camera gantry. The system was mounted on a 2-head camera with large open areas. The actual prototype requires a field width of 40 mm in the

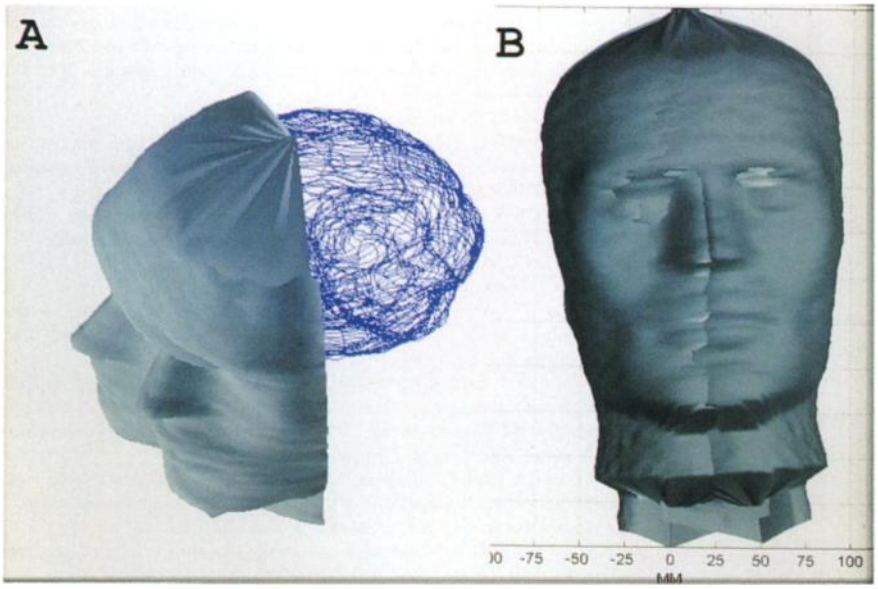

FIGURE 10. (A) Two masks of Oscar (and 1 SPECT, blue lines) plotted on 1 graph before merging process. (B) Three-dimensional rendering of 2 masks at 1 step of fusion process; significant difference remains between 2 masks.

FIGURE 11. At end of process resulting transformation matrix was applied to second set of brain SPECT data. Then 4 sets of data were plotted on same graph (light gray = mask 1 (reference set); red = SPECT slices 1 (reference set); dark gray = mask 2; yellow = SPECT slices 2.

transverse axis. Mounting it on a 3-head camera with close contact between the heads would require a different strategy.

One application for which this system is particularly suited is the merging of 2 sets of brain SPECT slices, an application used in this study as a test. Although these preliminary results were obtained by subjective manual action to merge the masks, it was remarkable that the rigid transformation applied to the SPECT slices worked well, at least on visual inspection. In the future, dedicated algorithms based on the work of Feldmar and Ayache (*13*) will be used.

The choice of the face (as a landmark) for image merging must be discussed. Indeed, information from the scalp or the skull is lacking. The patient lies in a supine position, with head on the rigid head holder. Under these conditions it can be hypothesized that the center of rotation of the patient's head will be located close to a point where it comes into contact with the head holder. In this case, the maximal motion amplitude will be found in the face, which also happens to be the most informative area for surface matching.

CONCLUSION

A new range finder, the conoscope, based on spatially incoherent interferometry, has been mounted on a 2-head γ camera and used to register the faces of an anthropomorphic test object and a volunteer, during a brain perfusion study. Among the various techniques that can be used for the purpose of image registration, the advantages of the conoscope are that it can yield directly an absolute value of the distance to the reference plane and its narrow 40-mm optical field, which could be useful for modality-to-patient registration procedures. Integrating the device to the γ-camera gantry allowed a robust calibration and will facilitate industrial implementation. Different mounting options or other scanning schemes (or both) will be investigated. Although the whole experiment must be reevaluated from an industrial viewpoint, our experimental results have shown the potential of the method for brain SPECT image registration, which was used as a reference test. Further work will provide more quantitative data required to evaluate the potential clinical usefulness of this new technique.

ACKNOWLEDGMENTS

This study was partially supported by the Hôpitaux Universitaires de Strasbourg, France. The authors thank Nathalie Heider for linguistic corrections.

REFERENCES

1. Zubal IG, Spencer SS, Khursheed I, et al. Differences images calculated from ictal and interictal technetium-99m-HMPAO SPECT scans of epilepsy. *J Nucl Med.* 1995;36:684–689.
2. Gottesfeld-Brown L. A survey of image registration techniques. *ACM Computing Surveys.* 1992;24:325–375.
3. Maintz JBA, Viergever MA. A survey of medical image registration. *Med Image Anal.* 1998;2:1–36.
4. Lavallée S. Registration for computed integrated surgery: methodology, state of the art. In: Taylor RH, Lavallée S, Burdea GC, Mösges R, eds. *Computer-Integrated Surgery, Technology and Clinical Applications.* Cambrigde, MA: MIT Press; 1996:77–97.
5. Sirat GY, Psaltis D. Conoscopic holography. *Opt Lett.* 1985;10:4–6.
6. Sirat GY, Psaltis D. Conoscopic holograms. *Opt Commun.* 1988;65:243–246.
7. Sirat GY, Malet Y. Conoscopic holography application: multipurpose rangefinders. *J Opt.* 1998;29:183–198.
8. Ettinger GJ, Leventon ME, Grimson WE, et al. Experimentation with a transcranial magnetic stimulation system for functional brain mapping. *Med Image Anal.* 1998;2:133–142.
9. Peria O, Lavallee S, Champleboux G, François-Joubert A, Lebas JF, Cinquin P. Millimetric registration of SPECT and MR images without head holders. In: *Proceedings of the IEEE EMBS San Diego conference.* San Diego, CA: Engineering Medical Biology Society; 1995:14–15.
10. Turkington TG, Jaszczak RJ, Pelizarri CA, et al. Accuracy of registration of PET, SPECT and MR images of a brain phantom. *J Nucl Med.* 1993;34:1587–1594.
11. Fitzpatrick JM, West JB, Maurer CR. Predicting error in rigid-body point-based registration. *IEEE Trans Med Imaging.* 1998;17;694–702.
12. Pelizzari CA, Chen TY, Spelbring DR, Weichselbaum RR, Chen CT. Accurate three-dimensional registration of CT, PET and/or MR images of the brain. *J Comput Assist Tomogr.* 1989;13:20–25.
13. Feldmar J, Ayache N. Rigid, afine and locally affine registration of free-form surfaces. *Int J Comput Vision.* 1996;18:99–119.